

Chapter 37

Fast Image Reconstruction Algorithm for Radio Tomographic Imaging

Zhenghuan Wang, Han Zhang, Heng Liu and Sha Zhan

Abstract Radio tomographic imaging is an emerging technology of imaging the attenuation by the objects in the area surrounded by the wireless sensor nodes to locate and track the objects. So it's significant to reconstruct the image in real-time to track the motion of the objects and also with good enough imaging quality. Tikhonov regularization can achieve the real-time requirement with acceptable imaging results by one-step multiplication. Landweber iteration can obtain better imaging quality but need many times of iteration. This paper use pre-iteration method to complete the iteration process of Landweber iteration offline and reconstruct the image online by one-step multiplication, just like Tikhonov regularization. Simulation and experiments show this method can get better imaging results than Tikhonov regularization and imaging the objects in real-time.

Keywords Radio tomographic imaging · Pre-iteration · Landweber iteration · Tikhonov regularization

37.1 Introduction

Radio tomographic imaging (RTI) is a new type of technology for location and tracking objects in the interesting area. Its basic idea is to deploy enough wireless sensor networks (WSNs) nodes surrounding the detection area [1]. If an object is located in the area, some links between the nodes which the radio signals travel

Z. Wang (✉) · H. Liu · S. Zhan
School of Information and Electronics, Beijing Institute of Technology,
Beijing, China
e-mail: wangzhenghuan@bit.edu.cn

H. Zhang
Beijing University of Posts and Telecommunications, Beijing, China

through will suffer great loss. Then an image which reflects the attenuation in the area is reconstructed with this technology. The bright spot is in the image where the object locates. RTI is a very appealing for security purpose because it works at radio bands which can penetrate wall and smoke with low power consumption. Other technologies either be blocked by walls or must have large transmitting power such as camera and radar. Another advantage of RTI is that it can utilize inexpensive nodes with small size, which can reduce the cost of the imaging system.

It is very significant to know the location of the objects in real-time, particularly for security areas. So the foremost aspect is that RTI must reconstruct the image fast enough to track the motion of the objects, followed by the localization precision or imaging quality. Image reconstruction of RTI is an ill-posedness problem. Some methods are used to solve this problem such as linear back projection (LBP), truncated singular value decomposition (TSVD), total variation (TV), Tikhonov regularization (TR), Landweber iteration (LI) [2–5]. LBP is very simple and can also achieve real-time imaging, but the quality of image is not quite good. TSVD and TV are too computational expensive to meet the requirement of real-time processing. TR is a good choice because this method can not only reconstruct the image real-time but also get acceptable imaging results. LI can achieve better imaging results than TR with finite iteration. This paper will use a pre-iteration method to complete the iteration process offline and reconstruct the image by one-step multiplication. So this method can not only retain the real-time characteristics as TR but also obtain better imaging results.

37.2 The Model of Radio Tomographic Imaging

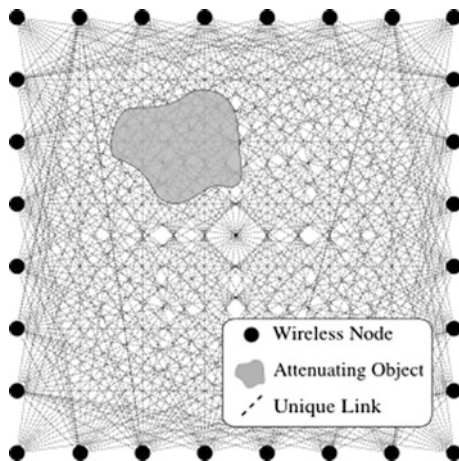
If K is the number of wireless sensor nodes deployed outside the imaging area as depicted in Fig. 37.1, when there is an object in the imaging area, some links will be blocked which means the signal will suffer great attenuation, usually up to 5–10 dB. Suppose P_i is received signal strength (RSS) of link i measured when there is an object in the area while P_i^e is RSS measured when the area is vacant. Their difference y_i is the shadowing loss of the link i caused by object's obstruction.

$$y_i = P_i - P_i^e \quad (37.1)$$

where the unit is dBm.

In order to obtain the image of attenuation when signal travels though the imaging area, the area is divided into many square regions with the same size and each small region is called a pixel. Suppose that the total number of pixels is N . x_j is the attenuation when the signal passes through the pixel j . Then y_i can be seen as the weighted sum of x_j [1].

Fig. 37.1 An illustration of radio tomographic imaging with wireless sensor network



$$y_i = \sum_{j=1}^N w_{ij}x_j + n_i \quad (37.2)$$

where n_i is the noise and w_{ij} is the weight of pixel j for link i .

w_{ij} can be determined by the ellipse model for each link in the network, which is very effective in outdoor environment.

$$w_{ij} = \frac{1}{\sqrt{d_i}} \begin{cases} 1 & \text{if } d_{ij}(1) + d_{ij}(2) < d_i + \delta \\ 0 & \text{otherwise} \end{cases} \quad (37.3)$$

where δ is a tunable parameter called ellipse parameter which describes the width of the ellipse, d_i is the distance between the two nodes, $d_{ij}(1)$ and $d_{ij}(2)$ are the distances between the center of pixel j and the two nodes for link i respectively.

In order to look more compact, (37.2) can be written in matrix form as

$$\mathbf{y} = \mathbf{w}\mathbf{x} + \mathbf{n} \quad (37.4)$$

where $\mathbf{y} = [y_1, y_2, y_3, \dots, y_M]^T \in R^M$ is shadowing loss vector, $\mathbf{w} = [w_{ij}]_{M \times N} \in R^{M \times N}$ is weight matrix, $\mathbf{x} = [x_1, x_2, x_3, \dots, x_N]^T \in R^N$ is pixel vector and $\mathbf{n} = [n_1, n_2, n_3, \dots, n_M] \in R^M$ is noise vector.

37.2.1 Tikhonov Regularization

Image reconstruction of radio tomographic imaging is an ill-posed problem because the number of pixels is much more than the number of RSS measurements in the wireless sensor network. TR might be the most popular method to solve the

ill-posed problem [1–3]. The standard TR is to minimize the following objective function.

$$\min_x \|y - wx\|^2 + \lambda \|x\|^2 \quad (37.5)$$

where λ is TR parameter. The solution of (37.5) is

$$\hat{\mathbf{x}}_{TR} = (\mathbf{w}^T \mathbf{w} + \lambda \mathbf{I})^{-1} \mathbf{w}^T \mathbf{y} \quad (37.6)$$

From the (37.6) it is quite clear that once λ is determined, the $(\mathbf{w}^T \mathbf{w} + \lambda \mathbf{I})^{-1} \mathbf{w}^T$ can be calculated in advance [1]. So the procedure of TR can be divided into two steps: one is get the $(\mathbf{w}^T \mathbf{w} + \lambda \mathbf{I})^{-1} \mathbf{w}^T$ offline and the other one is online image reconstruction by one step multiplication. That means real-time processing is possible, which is a very appealing feature of TR.

37.2.2 Landweber Iteration

Landweber iteration is widely used in some other image reconstruction areas such as ECT [3, 5]. It aims to minimize the following objective function in an iterative way.

$$f(\mathbf{x}) = \frac{1}{2} \|\mathbf{y} - \mathbf{w}\mathbf{x}\|^2 = \frac{1}{2} (\mathbf{y} - \mathbf{w}\mathbf{x})^T (\mathbf{y} - \mathbf{w}\mathbf{x}) \quad (37.7)$$

The steepest gradient descent method chooses the direction in which $f(\mathbf{x})$ as new search direction for next iteration [3]. This direction is opposite to the gradient of $f(\mathbf{x})$ at current point. The iteration procedure is therefore

$$\hat{\mathbf{x}}_{k+1} = \hat{\mathbf{x}}_k - \mu \nabla f(\hat{\mathbf{x}}_k) = \hat{\mathbf{x}}_k - \mu \mathbf{w}^T (\mathbf{w}\hat{\mathbf{x}}_k - \mathbf{y}) = (\mathbf{I} - \mu \mathbf{w}^T \mathbf{w}) \hat{\mathbf{x}}_k + \mu \mathbf{w}^T \mathbf{y} \quad (37.8)$$

where the constant μ is known as gain factor and is used to control convergence rate. The choice of μ will be explained later.

LI method needs many times of iteration before obtaining satisfying results, which is not suitable for on-line imaging.

37.2.3 Pre-iteration Landweber Iteration

In fact, the iteration task of LI can be undertaken offline. If $\mathbf{D} = \mathbf{I} - \mu \mathbf{w}^T \mathbf{w}$, then the equation can be rewritten as

$$\hat{\mathbf{x}}_{k+1} = \mathbf{D} \hat{\mathbf{x}}_k + \mu \mathbf{w}^T \mathbf{y} \quad (37.9)$$

The matrix \mathbf{D} is independent of \mathbf{x} and \mathbf{y} and it is an interesting feature of the LI method. Suppose that the initial value $\hat{\mathbf{x}}_0=0$, then after k iteration, the solution can be calculated as follows

$$\hat{\mathbf{x}}_k = (\mathbf{I} + \mathbf{D} + \mathbf{D}^2 + \mathbf{D}^3 + \dots + \mathbf{D}^{k-1})\mu\mathbf{w}^T\mathbf{y} = \mathbf{P}\mu\mathbf{w}^T\mathbf{y} \quad (37.10)$$

where $\mathbf{P} = (\mathbf{I} + \mathbf{D} + \mathbf{D}^2 + \mathbf{D}^3 + \dots + \mathbf{D}^{k-1})\mu\mathbf{w}^T$. Similar to TR, the coefficient matrix \mathbf{P} can be computed in advance and stored in the computer for real-time processing [6, 7]. Then the imaging process can be very simple, which just needs that the \mathbf{P} multiply the observed shadowing loss vector \mathbf{y} . Compared to TR, this method can not only keep the real-time performance that TR holds, but also achieve better imaging results than TR.

In (37.10) the iteration number k should be appropriately chosen because LI and PLI have the drawback of semi-convergence, which means the imaging quality deteriorates when k is larger than a certain number [3, 4, 8].

There is indeed an optimal iteration number k_0 existing to make the imaging error reach the minimum, but it's very difficult to determine. In most cases, k_0 is chosen empirically and it's sufficient to meet the requirement of most cases.

37.2.4 Calculation of \mathbf{P}

At the first glance it might be complex to compute \mathbf{P} because \mathbf{D} is a very large matrix with dimension $n \times n$ and the computation of \mathbf{P} requires a lot of time. In fact if we use some property of \mathbf{P} , the computation can be simplified substantially. Suppose that the singular value decomposition (SVD) of \mathbf{w} is $\mathbf{w} = \mathbf{U}\Sigma\mathbf{V}^H = \sum_{i=1}^r \sigma_i \mathbf{u}_i \mathbf{v}_i^H$ where $\mathbf{u}_i, \mathbf{v}_i, \sigma_i$ are the singular vector and singular value of \mathbf{w} respectively [9].

Then the SVD of \mathbf{D} and \mathbf{P} will be

$$\mathbf{D} = \mathbf{I} - \mu\mathbf{w}^T\mathbf{w} = \mathbf{V}(\mathbf{I} - \mu\Sigma^H\Sigma)\mathbf{V}^H = \mathbf{V}diag(1 - \mu\sigma_1^2, 1 - \mu\sigma_2^2, \dots, 1 - \mu\sigma_r^2)\mathbf{V}^H \quad (37.11)$$

$$\begin{aligned} \mathbf{P} &= (\mathbf{I} + \mathbf{D} + \mathbf{D}^2 + \mathbf{D}^3 + \dots + \mathbf{D}^{k_0-1})\mu\mathbf{w}^T = \mu\mathbf{V}diag\left(\sum_{k=0}^{k_0-1} (1 - \mu\sigma_1^2)^k, \sum_{k=0}^{k_0-1} (1 - \mu\sigma_2^2)^k, \dots, \sum_{k=0}^{k_0-1} (1 - \mu\sigma_r^2)^k\right)\mathbf{U}^H \\ &= \sum_{i=1}^r \frac{1 - (1 - \mu\sigma_i^2)^{k_0}}{\sigma_i} \mathbf{v}_i \mathbf{u}_i^H \end{aligned} \quad (37.12)$$

It can be seen that once SVD of the \mathbf{w} is completed and other parameters are determined, \mathbf{P} can be obtained immediately through (37.12).

From the (37.12), the principle of choosing μ can also be obtained. In order to guarantee the convergence, $1 - \mu\sigma_k^2$ should be less than 1. So the choice of μ should be $\mu < (1/\sigma_{\max}^2)$, where the σ_{\max} is the largest singular value of \mathbf{w} .

37.3 Results

37.3.1 Comparison of TR and PLI Using Simulated Data

It is obvious that the landweber iteration and Tikhonov regularization can complete the reconstruction by one-step processing. So their computational speed is the same. The only one aspect they may be different is the imaging quality.

The relative imaging error e is defined by

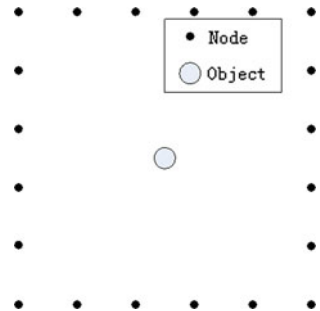
$$e = \frac{\|\mathbf{x} - \hat{\mathbf{x}}\|}{\|\mathbf{x}\|} \tag{37.13}$$

The true shadowing loss \mathbf{x} is obtained by simulation. We make the following assumption that shadowing loss of the links affected by object's obstruction is about 5 dB and the shadowing loss of other links is zero. The noise vector subject to Gaussian distribution and the variance is 0.8, $\mathbf{n} \sim N(0, 0.8)$.

The deployment of sensors is depicted in Fig. 37.2. The object is located at the center of the imaging area and modeled as a cylinder with radius of 10 cm. The imaging area is divided by 60*60 pixels and the size of each pixel 0.2 m*0.2 m, which means the numbers of elements in \mathbf{x} is 3600. The ellipse parameter σ , TR parameter λ and gain factor μ are chosen to be 0.03 m, 100 and 0.0001 respectively.

We can see the semi-convergence phenomenon of LI or PLI from the Fig. 37.3. At the beginning the relative imaging error decreases rapidly. After about 80 iterations, the relative imaging error reaches the minimum values and the corresponding error is 0.95. While when the iteration process continues, the relative imaging error increases and it's not difficult to guess that the imaging error will

Fig. 37.2 The simulation setting



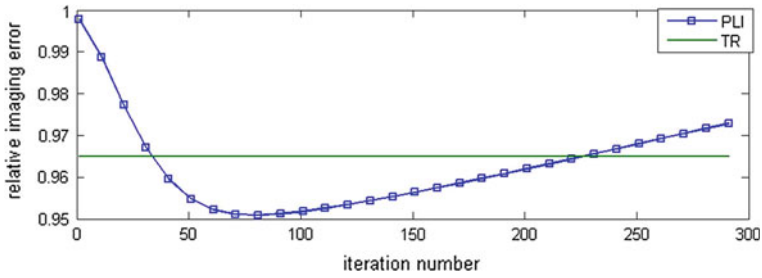


Fig. 37.3 The relative imaging error versus iteration number

converge to LS method when the iteration number reaches infinity. TR is not an iterative method, so its simulation curve is a straight line and the imaging error is 0.96 which is higher than LI or PLI. So we can conclude that PLI can achieve better imaging results than TR method.

37.3.2 Performance of PLI Using Experiments

To evaluate the performance of PLI method, the experiment was also conducted in outdoor environment. An area of 6 m × 6 m was monitored by 20 sensor nodes, as illustrated in Figs. 37.2 and 37.4. Each node was placed 1.2 m apart along the square perimeter of the monitored area and mounted on a tripod at a height of 1 m.

The nodes use JN5139 chip which is compatible with IEEE 802.15.4 protocol and operate at 2.4G frequency. A token ring protocol is utilized to avoid transmission collisions. During each time interval of 3 ms, one node broadcasted one packet. All the other nodes received the packet and measured the RSS of the packet. Then the token was passed to the next node in the next time interval. So the

Fig. 37.4 The experiment scenario



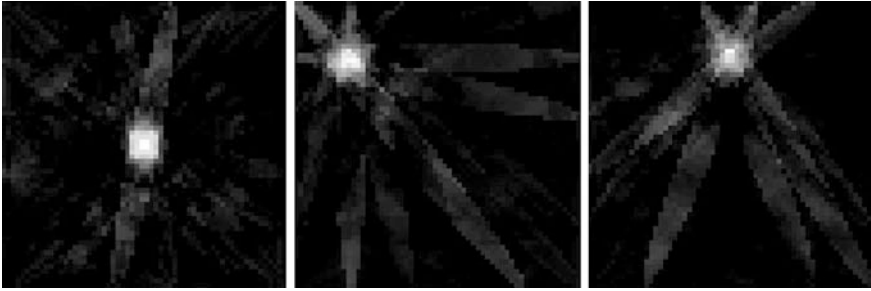


Fig. 37.5 The imaging results when one person locates the three positions

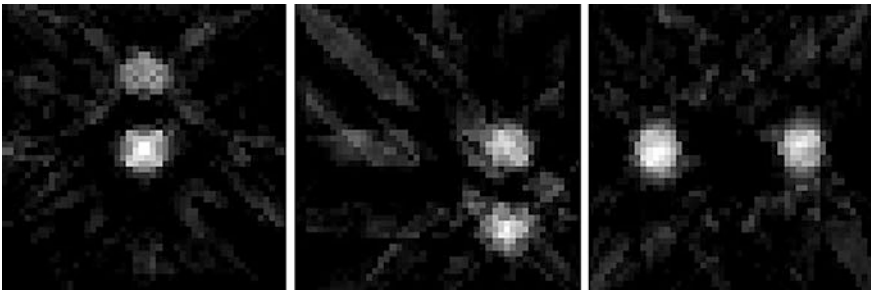


Fig. 37.6 The imaging results using PLI method when two persons locate in the monitored area

RSS on each link was updated every 60 ms. It's fast enough to track the motion of the targets in the area. The nodes sent the measured RSS data to the laptop. The laptop collected the data from the sensors and run the imaging software based on PLI in real-time

The values of parameters are the same with the simulation. Figure 37.4 shows the experiment scenario that a person was moving in the area in a norm speed. During the environment the person's location was shown real-time from the software.

Figure 37.5 shows the imaging results when person locating at three spots. From the images the person's position is clearly shown, which is the bright spot in the image.

In the model of RTI, it doesn't restrict the number of targets. In fact, RTI can also track multiple objects at the same time. Figure 37.6 shows the results when two persons moving in the monitored area using PLI method. It can be inferred when the two persons come too close, the results become a little worse and when the person stands far away, the results are much better.

37.4 Conclusion

This paper presents a pre-iteration landweber method to meet the real-time requirement of radio tomographic imaging. The PLI method can reconstruct the image by one-step multiplication, just like TR does while achieving better imaging results than TR. Simulation and experiment have demonstrated that PLI can locate and track the objects in real-time with enough precision.

Acknowledgments This work was supported in part by National Natural Science Foundation of China (No. 61101129, No. 61227001 and No. 60972017), Specialized Research Fund for the Doctoral Program of Higher Education (SRFDP) under Grant No.20091101110019 and No. 20091101120028.

References

1. Wilson, J., Patwari, N.: Radio tomographic imaging with wireless networks. *IEEE Trans. Mob. Comput.* **9**(5), 621–632 (2010)
2. Wilson, J., Patwari, N.: Regularization methods for radiotomographic imaging. In: *Proceedings of the Virginia Tech Symposium on Wireless Personal Communications (2009)*
3. Yang, W.Q., Peng, L.H.: Image reconstruction algorithms for electrical capacitance tomography. *Meas. Sci. Technol.* **14**, R1–14 (2003)
4. Peng, L.H., Mercus, H., Scarlett, B.: Using regularization methods for image reconstruction of electrical capacitance tomography. *Meas. Sci. Technol.* **17**, 96–104 (2000)
5. Yang, W.Q., Spink, D.M., York, T.A., McCann, M.: An image-reconstruction algorithm based on Landweber's iteration method for electrical-capacitance tomography. *Meas. Sci. Technol.* **10**, 1065–1069 (1999)
6. Liu, S., Fu, L., et al.: Prior-online iteration for image reconstruction with electrical capacitance tomography. *IEEE Proc. Sci. Meas. Technol* **151**(3), 195–200 (2004)
7. Wang, H., Wang, C., Yin, W.: A Pre-iteration method for the inverse problem in electrical impedance tomography. *IEEE Trans. Instrum. Meas.* **53**(4), 1093–1096 (2004)
8. Xiong, X.Y., Zhang, Z.T., Yang, W.Q.: A stable image reconstruction algorithm for EC. *J. Zhejiang Univ. Sci.* **6A**(12), 1401–1404 (2005)
9. Zhang, X.D.: *Matrix Analysis and Applications*. Tsinghua University Press, Beijing (2004)